CLEMENTI, E. & RAIMONDI, D. L. (1963). *J. Chem. Phys.* **38**, 2686–2689.
COPPENS, P., GURU ROW, T. N., LEUNG, P., STEVENS, E. D., BECKER, P. J. & YANG, Y. W. (1979). *Acta Cryst.* A**35**, 63–72.
COTTON, F. A. & WILKINSON, G. (1972). *Advanced Inorganic Chemistry*, 3rd ed. New York: Wiley.
CROMER, D. T. (1977). Private communication.
DOWNS, J. W., HILL, R. J., NEWTON, M. D., TOSSELL, J. A. & GIBBS, G. V. (1982). In *Electron Distributions and the Chemical Bond*, edited by P. COPPENS & M. B. HALL. New York: Plenum.
HANSEN, N. K. & COPPENS, P. (1978) *Acta Cryst.* A**34**, 909–921.
HEIJSER, W (1979). PhD Thesis. Free Univ., Amsterdam, Holland.
HOLLADAY, A. & COPPENS, P. (1983). In preparation.
International Tables for X-ray Crystallography (1974). Vol. IV. Birmingham: Kynoch Press.
IWATA, M. (1977). *Acta Cryst.* B**33**, 59–69.
IWATA, M. & SAITO, Y. (1973). *Acta Cryst.* B**29**, 822–832.
KURKI-SUONIO, K. (1977). *Isr. J. Chem.* **16**, 115–123.
LEUNG, P. & COPPENS, P. (1983). In preparation.
LEUNG, P., COPPENS, P., MCMULLAN, R. K. & KOETZLE, T. F. (1981). *Acta Cryst.* B**37**, 1347–1352.
MARTIN, M., REES, B. & MITSCHLER, A. (1982). *Acta Cryst.* B**38**, 6–15.
MOSS, G., HANSEN, N. K. & COPPENS, P. (1980). In *Computing in Crytallography*, edited by R. DIAMOND, S. RAMASESHAN & K. VENKATESAN. Bangalore: Indian Academy of Sciences.
ORTEGA, R. B. (1980). PhD Thesis. Univ. of New Mexico.
RAE, A. D. (1978). *Acta Cryst.* A**34**, 719–724.
REES, B. & COPPENS, P. (1973). *Acta Cryst.* B**29**, 2516–2528.
REES, B. & MITSCHLER, A. (1976). *J. Am. Chem. Soc.* **98**, 7918–7924.
ROSE, M. E. (1957). *Elementary Theory of Angular Momentum*. New York: Wiley.
STEVENS, E. D. & COPPENS, P. (1979). *Acta Cryst.* A**35**, 536–539.
STEWART, R. F. (1972). *J. Chem. Phys.* **57**, 1664–1668.
STEWART, R. F. (1976). *Acta Cryst.* A**32**, 565–574.
STEWART, R. F. (1977). *Chem. Phys. Lett.* **49**, 281–284.
SUMNER, G. G., KLUG, H. P. & ALEXANDER, L. E. (1964). *Acta Cryst.* **17**, 732–742.
WANG, Y. W. & COPPENS, P. (1976). *Inorg. Chem.* **15**, 1122–1127.
WEISS, R. J. & MAZZONE, G. (1981). *J. Appl. Cryst.* **14**, 401–416.

Acta Cryst. (1983). A**39**, 387–399

Dynamical X-ray Propagation: a Theoretical Approach to the Creation of New Wave Fields

BY F. BALIBAR

Laboratoire de Minéralogie–Cristallographie, associé au CNRS, Université Pierre et Marie Curie (Paris 6) et Paris 7, 4 place Jussieu, 75230 Paris CEDEX 05, France

F. N. CHUKHOVSKII

Institute of Crystallography, Academy of Sciences of the USSR, Moscow, USSR

AND C. MALGRANGE

Laboratoire de Minéralogie–Cristallographie, associé au CNRS, Université Pierre et Marie Curie (Paris 6) et Paris 7, 4 place Jussieu, 75230 Paris CEDEX 05, France

(*Received* 24 *February* 1982; *accepted* 2 *December* 1982)

Abstract

Although it is commonly invoked, the phenomenon of 'creation of new wave fields', which is responsible for some of the features visible on topographic images, has never been really explained in theoretical terms. This is done here in the case of a crystal deformed by a uniform strain gradient. The appropriate Green function is expanded in reciprocal space as a wave packet of non-plane waves, each component corresponding to a single value of the deviation parameter at the entrance surface. It is then shown that each component of this wave packet is made up of four parts, two of which can be identified as 'normal' wave fields (*i.e.* those predicted by the Eikonal theory); the two others are the so-called 'created wave fields'; it is shown that they correspond to interbranch scattering from one branch of the dispersion surface to the other and give rise to two extra beams. These created wave fields extract a fraction $e^{-2\pi|v|}$ out of the normal energy flow ($|v|$ being inversely proportional to the strain gradient), in full agreement with previous computer experiments.

I. Introduction

Understanding the so-called 'creation of new wave fields' in highly distorted parts of a crystal has been one

0567-7394/83/030387-13$01.50

of the major challenges of the dynamical theory of X-ray propagation, over the past 15 years. This phenomenon was first predicted on a theoretical basis by Penning (1966) in his thesis and was suggested by A. Authier in 1966 at the 15th Denver Conference on X-ray Analysis as an empirical explanation (Authier, 1967) for some of the features of the topographic image of a single dislocation: according to Authier, when travelling in a sufficiently distorted region, a given wave field (*i.e.* a set of two plane waves, represented by a *single* point P_i on the dispersion surface in reciprocal space) would give rise to two wave fields; one of them, the 'ordinary' wave field, being the expected continuation of the initial wave field (with a tie-point lying on the same branch of the dispersion surface as P_i), while the other, the 'newly created wave field', would propagate in a quite different, unexpected direction and would correspond to a tie-point lying on the opposite branch of the dispersion surface (this is the reason why this phenomenon is sometimes called 'interbranch scattering').

The idea of interbranch scattering already lies implicitly in the lamellar models proposed for the study of the propagation of X-rays in deformed crystals (Authier, 1961; Kato, 1963*a*). In these models the boundary conditions are applied at the interface between neighbouring slices.

Since then, this phenomenological statement has proved to be very useful as an empirical tool for the explanation of the observed images of certain types of defects (Authier, 1977). But no theoretical formulation of it has ever been given.

Clearly this phenomenon which contradicts the usual ray theory occurs when the Eikonal approximation (Kato, 1964; Penning, 1966) becomes invalid. Its theoretical treatment requires that the dynamical theory be expanded beyond the limits of applicability of the Eikonal approximation. This is, at least in principle, achieved by Takagi's (1969) theory which establishes the partial differential equations (along with the boundary conditions) to which the amplitude of the crystal wave must obey. If one takes into account the actual experimental resolution, this theory is valid for any strength of the deformation.

In contrast to the Eikonal theory, Takagi's treatment does not provide a direct analytical expression for the crystal wave. This latter is obtained as the convolution product of the amplitude distribution on the entrance surface (which depends on the form of the incident wave in vacuum) by the 'influence' or 'Green' function (which depends explicitly on the field of deformation in the bulk of the crystal). The mathematical difficulties involved are such that the influence function has been calculated only in some few cases (Chukhovskii, 1974; Katagawa & Kato, 1974; Litzman & Janacek, 1974). Among these is the case of a crystal with a uniform strain gradient; the influence function is then some confluent hypergeometric function. Although this, in principle, solves the problem of the propagation of an X-ray wave in such a medium, and therefore should account for the appearance of a 'recreated' wave field for large values of the strain gradient, all attempts to separate the 'ordinary' wave field from the 'recreated' one in the expression of the amplitude have failed up to now (Chukhovskii & Petrashen', 1977).

The reason for this is clear: the Green function which represents the influence of a single point P_0 (generally on the entrance surface) at another given point P (generally, on the exit surface) operates in *direct* space (or $\mathbf{r}$ space), while the concept of wave field belongs to a representation of the wave in *reciprocal* (or $\mathbf{K}$) space. A wave field is, by definition, a (single) point in reciprocal space. No wonder, then, that the Green function which is a function of $\mathbf{r}_P$ at P and $\mathbf{r}_{P_0}$ at P_0 does not provide a simple connection between the wave fields at the entrance surface and those at the exit surface. Clearly, this connection can be achieved only through an expansion of the Green function in reciprocal space.

The three following examples show that the Green function has to be expanded in reciprocal space in order to obtain information on the wave-field structure of the crystal wave.

(1) In the case of a perfect crystal, it is well known that the Green function is a Bessel function of zeroth order $J_0(\chi)$, where χ denotes some combination of the coordinates (both those of the point source P_0 and those of the point P where the field is to be calculated). Convoluting the amplitude distribution corresponding to an incident *plane* wave by this J_0, one would obtain the amplitude at P in the form of a sine function. Writing then this sine as a sum of two imaginary exponentials, one retrieves the usual wave fields 1 and 2 of the Ewald–Laue theory (Balibar, 1969*a*), as expected. But though the mathematical manipulation involved here [writing $\sin x$ as $(e^{ix} - e^{-ix})/2i$] is of the most trivial type, one still lacks physical reasons for doing so. Even in that case, the two wave fields come out of the Green function in a rather artificial manner.

(2) It would seem then, that separating the Green function itself into two parts would make the structure in wave fields appear more naturally. Since $J_0(\chi) = \frac{1}{2}[H_0^1(\chi) + H_0^2(\chi)]$ (where H_0^1 and H_0^2 are two Hankel functions), the expression for the amplitude at P is, for any shape of the incident wave, made up of two parts: one which is obtained through convolution of the incident amplitude distribution by H_0^1 and the other which involves H_0^2. Having shown that these two parts correspond, respectively, to a weakly absorbed mode, and a strongly absorbed mode, one of us (Balibar, 1968, 1969*b*, 1970) has proposed a description of the crystal wave in terms of 'generalized wave fields'. Apart from the fact that it relies on a

mathematical formula [$J_0 = \frac{1}{2}(H_0^1 + H_0^2)$] without any real physical meaning, this model does not provide any understanding of how the structure in **K** space of the crystal wave is related to that of the incident wave.

(3) Our last example is the work by Chukhovskii & Petrashen' (1977) where the procedure used in example (2) is extended to the case of a crystal with a uniform strain gradient. Having explicitly calculated the function which replaces J_0 in that case, these authors were able to represent it as a sum of two functions (the equivalent of the previous Hankel functions H_0^1 and H_0^2). But this separation, obtained by means of a general mathematical formula, still does not provide any understanding of how the **K** structure of the incident wave is transformed in the crystal. Nor does it show any 'creation of new wave fields' for sufficiently large values of the strain gradient.

In this paper we show that by a proper expansion of the Green function in reciprocal space (or **K** vectors space) the problem of how one wavefield can (for large values of the deformation) give two wave fields (*i.e.* two points in reciprocal space) can be solved. This treatment, which is performed for the case of a uniform strain gradient, could give some hints on how to deal with a more general type of deformation.

II. Expansion of the Green function as a wave packet (for a constant strain gradient)

Because of its (relative) simplicity, the case of a crystal with a uniform strain gradient has been extensively studied. Kato (1964) and Penning & Polder (1961) who have treated it on the basis of the Eikonal approximation (*i.e.* small strain gradient), have shown that the energy trajectories for the two wave fields induced by an incident plane wave are portions of hyperbolae, the characteristics of which depend on the values of the deformation and on the departure of the incident wave from Bragg's angle at the entrance surface. The general treatment, on the basis of Takagi's equations, has been performed by Chukhovskii (1974), Katagawa & Kato (1974), and Litzman & Janacek (1974) who all have given the exact analytical form of the influence function.

For reasons of simplicity, and after Chukhovskii & Petrashen' (1977), let us assume a transmission symmetric case and a constant strain gradient such that:

$$\mathbf{h}.\mathbf{u} = 4Bs_0 s_h$$
$$B = \frac{1}{4}\frac{\partial^2}{\partial s_0 \partial s_h}(\mathbf{h}.\mathbf{u}), \qquad (1)$$

where **h** = reciprocal-lattice vector (= 2π times the usual reciprocal-lattice vector = $2\pi\mathbf{h}_{\text{Kato}}$), **u** = atomic displacement, and s_0 and s_h are reduced coordinates in the transmitted and reflected directions (see Table 1 and Fig. 1).

The Green function for the reflected (h) wave is (see Chukhovskii & Petrashen', 1977):

$$G_h(P_0,P) = G_h[\mathbf{r}(P_0), \mathbf{r}(P)]$$
$$= [\Theta(\xi_h) - \Theta(-\xi_0)]\,{}_1F_1[-\nu,1;-4iB\xi_0\xi_h]. \qquad (2)$$

$\mathbf{r}(P_0)$ and $\mathbf{r}(P)$ are, respectively, the position vectors of

Table 1. *Comparison of the system of coordinates and deformation parameter used by different authors (symmetric case)*

	Kato	Penning & Polder	Chukhovskii and this paper
[h]/2 sin θ	$\frac{1}{\lambda}$	$\frac{1}{\lambda}$	$\frac{2\pi}{\lambda}$
Coordinate system	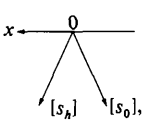	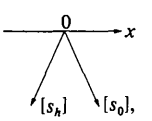	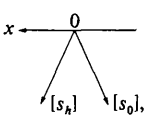
Coordinates along $\mathbf{K}_0$ and $\mathbf{K}_h$	$[s_0], [s_h]$	$[s_0], [s_h]$,	Reduced coordinates $s_0 = \frac{\pi}{\Lambda}[s_0]\cos\theta$ $s_h = \frac{\pi}{\Lambda}[s_h]\cos\theta$
Strain gradient	β_K	$\beta_P = -\beta_K$	$B = \frac{\Lambda}{2\pi}\beta_K$
Parameter $\lvert\eta\rvert$ at depth z	$\eta(z) = \eta(0) + \beta_K z$	$\eta(z) = \eta(0) - \beta_P z$	$\eta(z) = \eta(0) + \frac{2B\pi}{\Lambda}z$

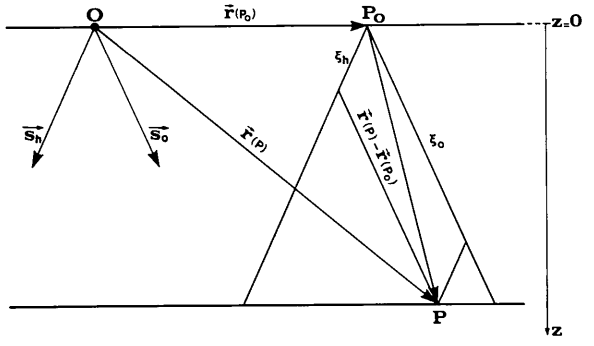

Fig. 1. Geometrical parameters in the case of a unit point source located at P_0 on the entrance surface. One calculates the wave $G_h(P_0,P)$ induced by such a source at $P(\xi_0, \xi_h)$ in the crystal.

a current point P_0 on the entrance surface and of the point P on the exit surface where the amplitude of the h wave is to be calculated (Fig. 1). Θ is the usual step function.

$$\xi_h = s_h(P) - s_h(P_0);$$
$$\xi_0 = s_0(P) - s_0(P_0);$$
$$\nu = \frac{i}{4B}; \tag{3}$$

${}_1F_1$ is the confluent hypergeometric function.

The Green function (2) can be expanded in reciprocal space by means of the Laplace transform, according to the following procedure. This is carried out here only on the term

$$\Theta(\xi_h)\,{}_1F_1(-\nu,1;-4iB\xi_0\,\xi_h)$$

since the calculation relative to

$$-\Theta(-\xi_0)\,{}_1F_1(-\nu;1;-4iB\xi_0\,\xi_h)$$

would be quite similar.

As a function of ξ_h (ξ_0 being considered as a parameter),

$$\Theta(\xi_h)\,{}_1F_1(-\nu,1;-4iB\xi_0\,\xi_h)$$

is expanded as (see *Higher Transcental Functions*, 1953):

$$\Theta(\xi_h)\,{}_1F_1(-\nu,1;-4iB\xi_0\,\xi_h) = \frac{1}{2\pi i}\int_{p_0-i\infty}^{p_0+i\infty} p^{-\nu-1}(p+4iB\xi_0)^{\nu}\,e^{p\xi_h}\,dp, \tag{4}$$

where p and ξ_h are conjugate variables relative to the Laplace transform.

Expressing in turn $(p + 4iB\xi_0)^{\nu}$ in terms of its inverse Laplace transform, one obtains:

$$\Theta(\xi_h)\,{}_1F_1(-\nu,1;-4iB\xi_o\,\xi_h) = \frac{1}{2\pi i}\int_0^{\infty} e^{-4iB\xi_0 t}\frac{t^{-\nu-1}}{\Gamma(-\nu)}\,dt\int_{p_0-i\infty}^{p_0+i\infty} e^{p(\xi_h-t)}\,p^{-\nu-1}\,dp = \int_0^{\xi_h} e^{-4iB\xi_0 t}\frac{t^{-\nu-1}}{\Gamma(-\nu)}\frac{(\xi_h-t)^{\nu}}{\Gamma(1+\nu)}\,dt$$

$$= \exp[-2iB(\xi_0+\xi_h)^2 + 2iB\xi_0^2]\int_0^{\xi_h} e^{4iB(\xi_0+\xi_h)(\xi_h-t)}\frac{(\xi_h-t)^{\nu}}{\Gamma(1+\nu)}\,e^{-2iB(\xi_h-t)^2}\frac{t^{-\nu-1}}{\Gamma(-\nu)}\,e^{2iBt^2}\,dt. \tag{5}$$

A second Laplace transform performed on this convolution product then leads (after some straightforward manipulation) to:

$$\Theta(\xi_h)\,{}_1F_1(-\nu,1;-4iB\xi_0\,\xi_h) = \frac{1}{2\pi i}\,e^{-i\pi\nu/2}\left(-\frac{i}{4B}\right)^{1/2}\exp[iB(\xi_0^2-\xi_h^2-2\xi_0\,\xi_h)]$$

$$\times\int_{p_0-i\infty}^{p_0+i\infty}\exp\left[\frac{p}{2}(\xi_h-\xi_0)\right]D_{\nu}\left[\left(\frac{i}{4B}\right)^{1/2}p\right]D_{-\nu-1}\left[\left(-\frac{i}{4B}\right)^{1/2}\{p-4iB(\xi_0+\xi_h)\}\right]dp, \tag{6}$$

where $D_{\nu}(z)$ is the parabolic cylinder function of order ν.

A similar calculation would show that:

$$\Theta(-\xi_0)\,{}_1F_1(-\nu,1;-4iB\xi_0\,\xi_h) = \frac{1}{2\pi i}\,e^{-i\pi(\nu+1)/2}\left(\frac{i}{4B}\right)^{1/2}\exp[iB(\xi_0^2-\xi_h^2-2\xi_0\,\xi_h)]$$

$$\times\int_{p_0-i\infty}^{p_0+i\infty}\exp\left[\frac{p}{2}(\xi_h-\xi_0)\right]D_{-\nu-1}\left[\left(-\frac{i}{4B}\right)^{1/2}p\right]D_{\nu}\left[\left(\frac{i}{4B}\right)^{1/2}\{p-4iB(\xi_0+\xi_h)\}\right]dp, \tag{7}$$

so that finally the Green function (2) is:

$$G_h(\xi_0,\xi_h) = \int_{p_0-i\infty}^{p_0+i\infty} P_h(p)\,dp, \tag{8}$$

where

$$P_h(p) = -\frac{1}{2\pi} e^{-i\pi\nu/2}\, v^{1/2} \exp[iB(\xi_0^2 - \xi_h^2 - 2\xi_0\xi_h)] \times \exp\left[\frac{p}{2}(\xi_h - \xi_0)\right] [D_\nu(-iY_0) D_{-\nu-1}(-Y) - D_{-\nu-1}(-Y_0) D_\nu(-iY)]. \tag{9}$$

The parameters Y_0 and Y introduced in (9) are such that

$$\left(\frac{i}{4B}\right)^{1/2} p = v^{1/2} p = -iY_0 \tag{10}$$

$$\left(\frac{i}{4B}\right)^{1/2} [p - 4iB(\xi_0 + \xi_h)] = v^{1/2}\left(p - \frac{4iB\pi z}{\Lambda}\right) = -iY \tag{11}$$

so that

$$Y = Y_0 + 4v^{1/2} B \frac{\pi}{\Lambda} z. \tag{12}$$

This should be compared to the well known formula relating the value of the deviation parameter η at a depth z to its value η_0 at the entrance surface:

$$\eta = \eta_0 + \frac{2B\pi}{\Lambda} z. \tag{13}$$

Let us recall that, in a symmetrical case, $\eta = \Delta\theta \sin 2\theta/(C\sqrt{\chi_h \chi_{\bar{h}}})$, where $\Delta\theta$ is the departure from Bragg angle, χ_h and $\chi_{\bar{h}}$ are the h and $\bar{h}$ Fourier coefficients of the electrical susceptibility and C is the polarization factor. Comparing (10), (12) and (13) leads to

$$p = -iv^{-1/2} Y_0 = -2i\eta_0 \tag{14}$$

with

$$Y(z) = 2v^{1/2}\eta(z). \tag{15}$$

Equation (14) shows that the variable of integration in (8) is directly proportional to the deviation parameter η_0 at the entrance surface. The interpretation of $P_h(p)$ then becomes clear: if one expands the spherical wave (which on the vacuum side of the entrance surface represents a unit point source at P_0) as a sum of plane waves (each being characterized by a single value of p or, alternatively, η_0, then $P_h(p)$ is the wave induced in the crystal at a point $P(\xi_0,\xi_h)$ by the component p of this expansion In other words: each of the vacuum plane-wave components is transformed, through the crystal, in $P_h(p)$. Integrating $P_h(p)$ over all values of p then gives the field at P due to a unit point source at $P_0(0,0)$; in other words, the Green function $G_h(\xi_0,\xi_h)$.

III. Analytic expression of each component $P_h(p)$ as a function of the deviation parameter

Since we are interested here in the phenomenon of 'creation' of 'new' wave fields, the analytic form of $P_h(p)$ will be calculated assuming a situation for which this phenomenon is expected. According to an argument first stated by Penning & Polder (1961), this 'creation' is most likely to occur at a depth $z = z_0$ such that $\eta(z_0) = 0$, since the curvature of the ray trajectory is then at its maximum. This conjecture has been amply verified by a computer experiment performed on the basis of Takagi's equations (Balibar, Epelboin & Malgrange, 1975). In this same computer experiment, the value of $|B|$ for which 'creation' becomes noticeable has been estimated: $4|B|$ must be of the order of 3 so that 10% of the total intensity be diverted in the 'created' wave fields. This result is in agreement with the criterion previously given by Balibar (1970) on a theoretical basis: creation of new wave fields is expected for $4|B| \gg 1$. We shall, therefore, from now on, assume:

(1) $|B| \gg 1$ and, for instance, $B > 0$. (A positive value of B corresponds to the geometry of Fig. 2.)

(2) The plane $z = z_0$ [such that $\eta(z_0) = 0$] lies *inside* the crystal (see Fig. 2). For a positive value of B, this imposes a large and negative value for $\eta_0 = \eta(0)$. *A priori*, we expect that for $z < z_0$ the crystal wave will be of the 'normal' type (*i.e.* only two wave fields) while for $z > z_0$ it will exhibit two extra terms.

The assumed conditions and their implications regarding the various parameters involved are

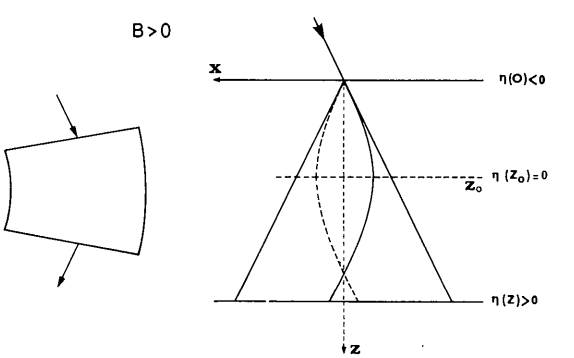

Fig. 2. Geometry of the crystal deformation in the case $B > 0$. Creation of a new wave field is expected to occur in the region $z \simeq z_0$ where the curvature of the ray trajectory is a maximum $[\eta(z_0) = 0]$.

summarized below:

(1) B large and $>0 \Rightarrow |\nu| = \left|\frac{i}{4B}\right| \ll 1 \quad \nu = |\nu| e^{i\pi/2}$; (16)

(2) $\eta_0 = \eta(0)$ large and $<0 \Rightarrow Y_0 = |Y_0| e^{5i\pi/4}$; (17)

(3) $\eta(z) = \eta(0) + 2\pi \frac{B}{A} z$ large and >0 $(z > z_0)$

$\Rightarrow Y = |Y| e^{i\pi/4}$. (18)

Under these conditions $P_h(p)$ at a given point (ξ_0, ξ_h) is (see Table 2):

$$P_h(p) = \exp[iB(\xi_0^2 - \xi_h^2 - 2\xi_0\xi_h)] \exp\left[\frac{p}{2}(\xi_h - \xi_0)\right] \times \left\{ \nu^{1/2} \frac{1}{2\pi} \left(\frac{Y_0}{Y}\right)^{\nu} \frac{1}{Y} \exp[\tfrac{1}{4}(Y_0^2 - Y^2)] - e^{2i\pi\nu}\, \nu^{1/2} \frac{1}{2\pi} \left(\frac{Y}{Y_0}\right)^{\nu} \frac{1}{Y_0} \exp[\tfrac{1}{4}(Y^2 - Y_0^2)] - e^{i\pi/4} e^{-3i\pi\nu/2} (1 - e^{2i\pi\nu})^{1/2} \frac{1}{2\pi} (YY_0)^{\nu} \times \exp[\tfrac{1}{4}(Y^2 + Y_0^2)] - e^{-i\pi/4} e^{3i\pi\nu/2} (1 - e^{2i\pi\nu})^{1/2}\, \nu \frac{1}{2\pi} (YY_0)^{-\nu-1} \times \exp[-\tfrac{1}{4}(Y^2 + Y_0^2)] \right\}. \quad (19)$$

As conjectured, $P_h(p)$ is a sum of four terms, A, B, C, D:

$$A = \frac{1}{2\pi} \exp[iB(\xi_0^2 - \xi_h^2 - 2\xi_0\xi_h)] \times e^{p/2(\xi_h - \xi_0)} |\nu|^{1/2} \left|\frac{Y_0}{Y}\right|^{\nu} \frac{1}{|Y|} e^{i/4(|Y_0|^2 - |Y|^2)} e^{-\pi|\nu|} \quad (20a)$$

Table 2. *Asymptotic expansion of the parabolic cylinder functions D_ν for large values of the argument u*

Parabolic cylinder functions D_ν

$$D_\nu(u) = u^\nu e^{-u^2/4} - \frac{\sqrt{2\pi}}{\Gamma(-\nu)} u^{-\nu-1} e^{u^2/4}\, \varepsilon_\nu(u),$$

where $\varepsilon_\nu(u)$ depends on the argument χ of u.

$$-\frac{3\pi}{4} < \chi < \frac{3\pi}{4} \quad \varepsilon_\nu(u) = 0$$

$$\frac{\pi}{4} < \chi < \frac{5\pi}{4} \quad \varepsilon_\nu(u) = e^{i\pi\nu}$$

$$-\frac{5\pi}{4} < \chi < -\frac{\pi}{4} \quad \varepsilon_\nu(u) = e^{-i\pi\nu}$$

$$B = \frac{1}{2\pi} \exp[iB(\xi_0^2 - \xi_h^2 - 2\xi_0\xi_h)] \times e^{p/2(\xi_h - \xi_0)} |\nu|^{1/2} \left|\frac{Y}{Y_0}\right|^{\nu} \frac{1}{|Y_0|} e^{i/4(|Y|^2 - |Y_0|^2)} e^{-\pi|\nu|} \quad (20b)$$

$$C = -\frac{1}{2\pi} \exp[iB(\xi_0^2 - \xi_h^2 - 2\xi_0\xi_h)]\, e^{p/2(\xi_h - \xi_0)} \times e^{i\pi/4} (|Y||Y_0|)^{\nu}\, e^{i/4(|Y|^2 + |Y_0|^2)} (1 - e^{-2\pi|\nu|})^{1/2} \quad (20c)$$

$$D = \frac{1}{2\pi} \exp[iB(\xi_0^2 - \xi_h^2 - 2\xi_0\xi_h)] \times e^{p/2(\xi_h - \xi_0)}\, e^{-i\pi/4} |\nu| (|Y||Y_0|)^{-\nu-1} \times e^{-i/4(|Y|^2 + |Y_0|^2)} (1 - e^{-2\pi|\nu|})^{1/2}. \quad (20d)$$

Correlatively, $G_h(P_0, P)$ is a sum of four integrals.

Note that this conclusion holds only under the conditions [see (17)–(18)] that Y and Y_0 be of opposite signs. It can be easily shown that if Y and Y_0 were of the same sign, *i.e.* if the conditions $\eta(z) = 0$ were not fulfilled *inside* the crystal, then $P_h(p)$ in (19) would reduce to only two terms – as expected.

IV. Physical interpretation – 'creation' of new waves

At this stage one would like to follow Kato's procedure and obtain the physical interpretation of the four terms involved in (20) by means of the stationary-phase method (Kato, 1961).

Let us call φ_A, φ_B, φ_C and φ_D the phases in (20*a*), (20*b*), (20*c*) and (20*d*), respectively. They can be written, using (10) and (11), as:

$$\varphi_A = -2iB\xi_h^2 - 4iB\xi_0\xi_h + p\xi_h$$

$$\varphi_B = 2iB\xi_0^2 - p\xi_0$$

$$\varphi_C = 2iB\xi_0^2 - p\xi_0 - \frac{ip^2}{8B}$$

$$\varphi_D = -2iB\xi_h^2 - 4iB\xi_0\xi_h + p\xi_h + \frac{i}{8B} p^2. \quad (21)$$

Unfortunately, it turns out that integration by the stationary-phase method can be performed only on φ_C and φ_D since the phases φ_A and φ_B cannot be made stationary owing to their linearity in p. We shall therefore use the stationary-phase method for C and D only and another method for A and B.

A. *The normal part of $G_h(P_0, P)$*

The phases φ_C and φ_D are stationary for

$$p^*_{[1]} = 4iB\xi_0 \quad \text{and} \quad p^*_{[2]} = 4iB\xi_h, \quad (22)$$

respectively.

The corresponding values of η_0 are:

$$\eta^*_{0[1]} = -2B\xi_0 \quad \text{and} \quad \eta^*_{0[2]} = -2B\xi_h. \tag{23}$$

Comparison with (*A*.1.3) and (*A*.1.4) in Appendix 1 shows that these values of η_0 are precisely those which would characterize the two hyperbolic trajectories which, according to the Eikonal theory, link $P_0(0,0)$ to $P(\xi_0,\xi_h)$ in the limit $B \gg 1$ and $|\eta_0|$ and $|\eta_p| \gg 1$.

In other words: in the case $B \gg 1$, the 'normal' part of $G_h(P_0,P)$ is zero everywhere except along the trajectories (see Fig. 10) along which energy is normally transferred in the case $B \ll 1$. This is, of course, the reason why we call this part of $G_h(P_0,P)$ the 'normal' one.

B. *The 'non-normal' part of* $G_h(P_0,P)$

We call 'non-normal' what is left once the 'normal' part has been taken into account:

$$\int_{p_0-i\infty}^{p_0+i\infty} \exp[iB(\xi_0^2 - \xi_h^2 - 2\xi_0\,\xi_h)]\, e^{p/2(\xi_h-\xi_0)} \times \frac{\nu^{1/2}}{2\pi}\left(\frac{Y_0}{Y}\right)^{\nu}\frac{1}{Y}\exp[\tfrac{1}{4}(Y_0^2 - Y^2)]\,dp \tag{24a}$$

and

$$\int_{p_0-i\infty}^{p_0+i\infty} \exp[iB(\xi_0^2 - \xi_h^2 - 2\xi_0\,\xi_h)]\, e^{p/2(\xi_h-\xi_0)}\, e^{2i\pi\nu} \times \frac{\nu^{1/2}}{2\pi}\left(\frac{Y}{Y_0}\right)^{\nu}\frac{1}{Y_0}\exp[\tfrac{1}{4}(Y^2 - Y_0^2)]\,dp \tag{24b}$$

or, alternatively (upon replacement of Y_0 and Y by their expression as functions of p):

$$\frac{1}{2\pi}\exp(-2iB\xi_h^2 - 4iB\xi_0\,\xi_h) \times \int_{p_0-i\infty}^{p_0+i\infty} p^{\nu}[p - 4iB(\xi_0+\xi_h)]^{-\nu-1}\, e^{p\xi_h}\,dp \tag{25a}$$

and

$$\frac{1}{2\pi}\exp(2iB\xi_0^2)\, e^{2i\pi\nu} \times \int_{p_0-i\infty}^{p_0+i\infty} p^{-\nu-1}[p - 4iB(\xi_0+\xi_h)]^{\nu}\, e^{-p\xi_0}\,dp. \tag{25b}$$

As already mentioned, integration by the stationary-phase method is not possible. Nevertheless, (25*a*) and (25*b*) can be calculated directly using the properties of the Laplace transform (see *Higher Transcendental Functions*, 1953), which gives for (25*a*)

$$i\exp(2iB\xi_h^2)\,{}_1F_1[-\nu,1;-4iB(\xi_0+\xi_h)\,\xi_h]\,\Theta(\xi_h) \tag{26a}$$

and for (25*b*)

$$-i\,e^{2i\pi\nu}\exp(2iB\xi_0^2)\,{}_1F_1[-\nu,1;-4iB(\xi_0+\xi_h)\,\xi_0]\,\Theta(\xi_0). \tag{26b}$$

The same ${}_1F_1$ function as in $G_h(P_0,P)$ appears [see equation (2)] except that the argument $\xi_0\,\xi_h$ has to be replaced either by $(\xi_0+\xi_h)\,\xi_h$ in (26*a*) or $(\xi_0+\xi_h)\,\xi_0$ in (26*b*). Expression (26*a*), for instance, is then calculated following the procedure which led from (4) to (8) and (9), ξ_0 being replaced by $(\xi_0+\xi_h)$ and ξ_h unchanged. One then obtains for the integrand, in the limit $\nu \to 0$ and $|Y_0|$ and $|Y| \gg 1$, a sum of four terms analogous to (20*a*)–(20*d*). It will be shown in the following section that, among these four terms, (20*c*) is predominant. Since the phase of this major term varies quadratically with p, it can be integrated using the stationary-phase method. The stationary condition is similar to (22) and (23) except that ξ_0 has to be replaced by $(\xi_0+\xi_h)$; this gives

$$p'^*_{[1]} = 4iB(\xi_0+\xi_h) \quad \text{or} \quad \eta'^*_{0[1]} = -2B(\xi_0+\xi_h). \tag{27}$$

The corresponding optical path (Fig. 3) is a broken line made of two straight segments, similar to that of the normal [1] wave field except that the turning point is now defined by $P_0\,S'_{[1]} = (\Lambda/\pi\cos\theta)(\xi_0+\xi_h)$ so that $S'_{[1]}$ coincides with A, the limit of the Borrmann fan on the exit surface. We therefore come to the conclusion that *the 'non-normal' part* (26*a*) *of* $G_h(P_0,P)$ *is zero everywhere except along* $\mathbf{s}_0$. A similar procedure would show that the 'non-normal' part (26*b*) of $G_h(P_0,P)$ is

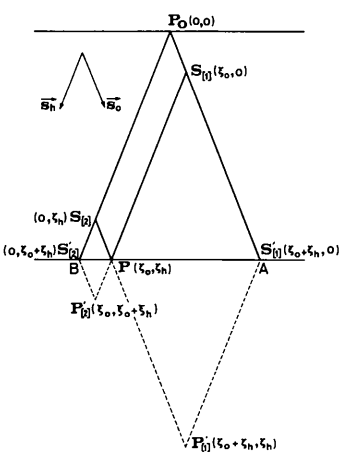

Fig. 3. Energy distribution in the crystal due to a unit point source P_0. A fraction of the energy is normally transferred to every point P of the exit surface along the two normal trajectories $P_0S_{[1]}P$ and $P_0S_{[2]}P$. The rest propagates 'non-normally', *i.e.* for each P, it propagates as if it were going to be normally transferred to two virtual points $P'_{[1]}$ and $P'_{[2]}$ lying outside the crystal. As a consequence, the non-normally transmitted part of the energy emitted by P_0 propagates in the crystal, parallel to $\mathbf{s}_0$ and $\mathbf{s}_h$, along the two edges of the Borrmann fan.

zero everywhere except along $\mathbf{s}_h$. For this second extra wave:

$$p'^{*}_{[2]} = 4iB(\xi_0 + \xi_h) \quad \text{or} \quad \eta'^{*}_{0[2]} = -2B(\xi_0 + \xi_h). \quad (28)$$

V. Energy flow of an incident pseudo plane wave. Interbranch scattering

Let us now consider an incident pseudo plane wave, *i.e.* a plane wave of finite lateral expansion (see Appendix 1). Let η_0 be its characteristic deviation parameter at the entrance surface. $G_h(P_0,P)$ has been expressed in (8) as an integral over p or alternatively over η_0 as $p = -2i\eta_0$; therefore the integrand in (8), $P_h(p) = P_h(-2i\eta_0)$, can be considered as representing the wave which is induced in the crystal by the considered pseudo plane wave. This conjecture is confirmed by the fact that the phases of the normal parts of $P_h(p)$ are identical to the Eikonal calculated in Appendix 1 [compare φ_C and φ_D in (21) with (*A*.1.12)].

Let us now study in more detail the four terms A, B, C and D involved in $P_h(p) = A + B + C + D$ [equation (20)].

A. Energy trajectories

In the previous section we have shown how the energy of a unit point source (*i.e.* an incident spherical wave) is distributed inside the crystal. These results are pictured on the left side of Fig. 4 where 4(*c*) corresponds to $|B| \ll 1$ and 4(*e*) to $|B| \gg 1$. The main difference between 4(*e*) and 4(*c*) is that in the case $|B| \gg 1$ new energy flow trajectories appear on the edges of the Borrmann fan and only there (§ IV). From this, one can infer the energy flow inside the crystal for an incident pseudo plane wave in the case $|B| \gg 1$ (Fig. 4*f*) from the case $|B| \ll 1$ (Fig. 4*d*). The conclusion is that an incident pseudo plane wave induces four wave fields inside the crystal; two of these are 'normal', and the other two are the so-called 'recreated wave fields'.

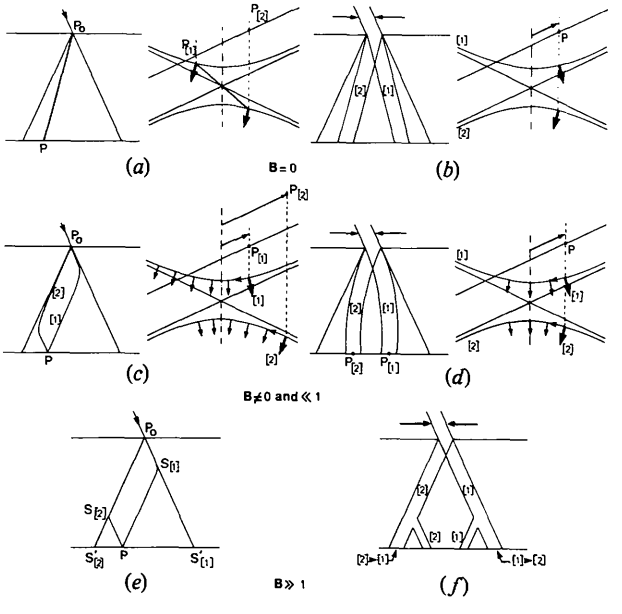

Fig. 4. Wave propagation in a crystal, assuming: *left*: an incident spherical wave (*a*,*c*,*e*); *right*: an incident pseudo plane wave (*b*,*d*,*f*). (*a*),(*b*) A perfect crystal $B = 0$. (*c*),(*d*) A slightly distorted crystal $|B| \neq 0$ and $|B| \ll 1$. (*e*),(*f*) A highly distorted crystal $|B| \gg 1$.

B. Intensity splitting

The intensities of these four wave fields are obtained by squaring the amplitudes A, B, C and D in (20).

In the limit $|v| \to 0$ this gives:

$$I_A \simeq 1 \times e^{-2\pi|v|} \times \frac{1}{4\eta^2}$$

$$I_B \simeq \frac{1}{4\eta_0^2} \times e^{-2\pi|v|} \times 1$$

$$I_C \simeq 1 \times (1 - e^{-2\pi|v|}) \times 1$$

$$I_D \simeq \frac{1}{4\eta_0^2} \times (1 - e^{-2\pi|v|}) \times \frac{1}{4\eta^2}. \quad (29)$$

The intensities have been written in this peculiar form on purpose, in order to evidence three successive splittings of the intensity during propagation:

(*a*) Remembering (see Appendix 2) that at the entrance surface the incident beam (of intensity normalized to 1) corresponding to a pseudo plane wave of deviation parameter η_0 is split into two wave fields, of respective intensities $1/4\eta_0^2$ and $1 - (1/4\eta_0^2) \simeq 1$ (as $|\eta_o|$ is large), we can interpret the first factor in each of the four intensities (29) as representing the splitting of the incident intensity between the two wave fields at the entrance surface. I_A and I_C thus pertain to the same wave field (wave field [1] if $B > 0$) while I_B and I_D should be associated with the other.

(*b*) These wave fields propagate normally (*i.e.* according to hyperbolic trajectories which in the case $|B| \gg 1$ reduce to broken lines) up to a region at a depth z_0 such that $\eta(z_0) \simeq 0$, where, as already shown creation of new wave fields occurs. The second factor in the intensities (29) indicates how the intensity of a given wave field is then shared between the normal and the created wave fields. For instance, the wave field which propagates with an intensity $1/4\eta_0^2$ in the region $z < z_0$ (see I_B and I_D) is split in the region $z \simeq z_0$ into two parts of relative intensities $e^{-2\pi|v|}$ (extra wave field) and $(1 - e^{-2\pi|v|})$ (normal wave field).

(*c*) The third factor in each term of (29) represents the splitting of the intensity at the exit surface for each of the four wave fields which propagate in the region

$z > z_0$. η, the deviation parameter at the exit surface, is the same for all four wave fields which means that equation (13) holds for new wave fields as well. This discussion is summarized in Fig. 5.

C. *Interbranch scattering*

The question now is: 'Do the extra wave fields correspond to interbranch scattering?' (interbranch meaning a 'jump' of the tie-point from one branch to the other in the process of the creation of a new wave field at $z \simeq z_0$).

This question can be answered by consideration of the phases involved in (20). Except for a factor $B(\xi_0^2 - \xi_h^2 - 2\xi_0\xi_h) - \eta(\xi_h - \xi_0)$ these phases are:

$$\varphi_A = \frac{1}{4|B|}(\eta_0^2 - \eta^2)$$

$$\varphi_B = \frac{1}{4|B|}(\eta^2 - \eta_0^2)$$

$$\varphi_C = \frac{1}{4|B|}(\eta_0^2 + \eta^2)$$

$$\varphi_D = \frac{1}{4|B|}(-\eta_0^2 - \eta^2). \qquad (30)$$

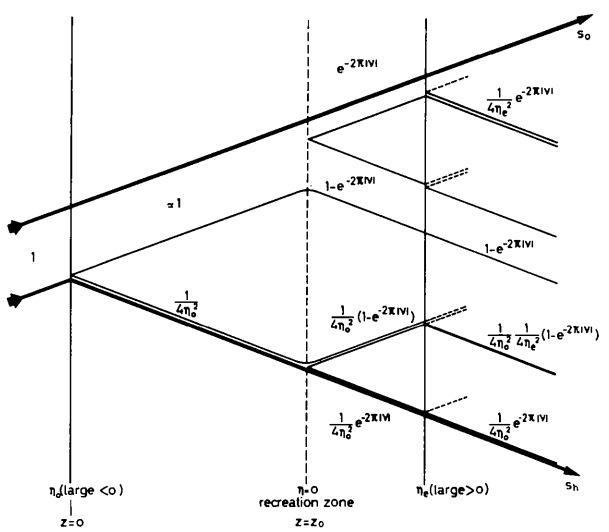

Fig. 5. Propagation of a pseudo plane wave inside a crystal distorted by a constant strain gradient $|B| \gg 1$ (here: $B > 0$). η_0, the value of the deviation parameter at the entrance surface, is large and negative. η then varies monotonically with the depth z inside the crystal. At $z = z_0$, η reaches the value $\eta = 0$, the curvature of the wave field is the maximum and new wave fields are 'created'; each new wave field takes a fraction $e^{-2\pi|V|}$ of the intensity of the wave from which it is 'created'. The splitting of the intensity among the two wave fields at the entrance surface, and among the refracted and reflected wave at the exit surface, is in agreement with the results of the ordinary dynamical theory (as long as one considers that the variations of η follows the same laws as in a slightly distorted crystal).

As can be seen from (*A*.1.12) in Appendix 1, a + sign in front of η^2 (respectively η_0^2) corresponds to a wave field of type [1] while a − sign is characteristic of a type [2] wave field.

Therefore, the tie-points of 'normal wave fields' [*C* and *D* in (20)] stay on the same branch of the dispersion surface (see in Fig. 6 the black arrows going from *M* to *R* for wave field [1], for example, which corresponds to the *C* term). The 'extra wave fields' [*A* and *B* in (20)] exhibit a mixed dependence $(\eta_0^2/4|B|) - (\eta^2/4|B|)$ or $(-\eta_0^2/4|B|) + (\eta^2/4|B|)$. The *A* term corresponds to a tie-point on branch [1] $(+\eta_0^2/4|B|)$, which upon arrival at region $z \simeq z_0$, jumps to branch [2] $(-\eta^2/4|B|)$ – see black arrows from *M* to *N* followed by white arrows from *P* to *Q* after the jump from *N* to *P*. This term is responsible for the interbranch scattering from branch [1] to branch [2]. Similarly the *B* term takes into account interbranch scattering from branch [2] to branch [1].

This argument can be stated more precisely by comparing the phase φ_A (or φ_B) with the Eikonal along the corresponding trajectory of mixed [1] and [2] type.

Let us consider, as in Fig. 7, a wave field of type [1] which, after the turning point $S_{[1]}$ where $\eta = 0$, splits into a normal wave field (trajectory $S_{[1]}P$) and a newly

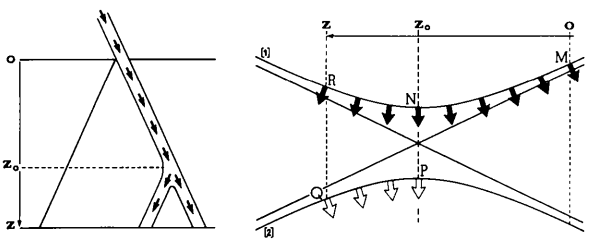

Fig. 6. Interbranch scattering (only one wave field, here [1], has been pictured for clarity). At a depth $z \simeq z_0$, the wave field which from $z = 0$ to z_0 propagates as a type [1] wave field (black arrows from *M* to *N*), splits into two waves, one of type [1] (black arrows from *N* to *R*) and one of type [2] (white arrows from *P* to *Q*).

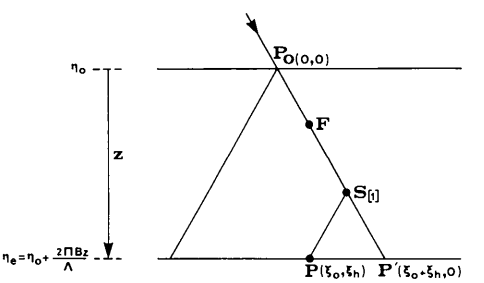

Fig. 7. Schematic drawing showing the ray paths corresponding to interbranch scattering. A normal wave field (here of type [1]) follows $P_0S_{[1]}$ and then splits into two wave fields: a normal one propagating along $S_{[1]}P$ and a new one (here of type [2]) propagating along $S_{[1]}P'$.

created wave field (trajectory $S_{[1]}P'$). The phase change along $P_0 S_{[1]}P'$ is, from (20),

$$\varphi_A = B(\xi_0'^2 - \xi_h'^2 - 2\xi_0'\xi_h') - \eta_0(\xi_h' - \xi_0') + \frac{\eta_0^2}{4|B|} - \frac{\eta^2}{4|B|}, \tag{31}$$

where ξ_0' and ξ_h' are the coordinates of P', *i.e.*

$$\begin{aligned} \xi_0' &= \xi_0 + \xi_h \\ \xi_h' &= 0 \end{aligned} \tag{32}$$

if ξ_0 and ξ_h are the coordinates of P. B is assumed to be positive.

Let us check that (31), along with (32), is identical to the Eikonal which would correspond to a wave field of type [1] from P_0 to $S_{[1]}$ and then a wave field of type [2] from $S_{[1]}$ to P'. The Eikonal φ_1 along $P_0 S_{[1]}$ and φ_2 along $S_{[1]}P'$ can be calculated from (A.1.12) which gives the phase φ_j along a wave field j propagating from $P_0(0,0)$ to $P(\xi_0, \xi_h)$. Then

$$\varphi_1 = B\xi_0^2 + \eta_0\xi_0 + \frac{\eta_0^2}{4B}, \tag{33}$$

as $\eta = 0$, $\xi_0(S_{[1]}) = \xi_0$, $\xi_h(S_{[1]}) = 0$. φ_2 along $S_{[1]}P'$ is equal to the phase along a wave field 2 going from P_0 to F:

$$\varphi_2 = B\xi_h^2 - \frac{\eta^2}{4B} \tag{34}$$

as $\eta_0 = 0$, $\xi_0(F) = \xi_h$, $\xi_h(F) = 0$. Adding (33) and (34) gives (31) once ξ_0' and ξ_h' have been replaced by their values (32) and (A.1.3) used.

D. The scattering factor; comparison with previous computer experiments

As has been stated in § V B, when creation occurs, the new wave field takes a fraction $e^{-2\pi|\nu|}$ out of the initial intensity, leaving a fraction $(1 - e^{-2\pi|\nu|})$ in the beam which keeps going normally. We call this factor $e^{-2\pi|\nu|}$ the scattering factor since the phenomenon here is quite analogous to a scattering process.

This quantity is of importance and it can be related to computer experiments performed by Balibar, Epelboin & Malgrange (1975). They have calculated (by numerical integration of Takagi's equations) the transmitted and reflected intensities by a crystal distorted with a constant strain gradient, assuming a pseudo plane wave and no absorption. The results showed that new wave fields appear for values of $B \gg 1$ and in the region $z \simeq z_0$ where $\eta(z_0) = 0$.

The intensity I_N of the new wave field, as compared to that of the incident intensity I_0, was empirically shown, from the numerical results obtained, to be of the type:

$$\frac{I_N}{I_0} = \exp\left(-\frac{\alpha}{B}\right) \tag{35}$$

where α was a constant.

The present work, apart from the fact that it provides a theoretical explanation of these 'experimental' results, allows one to give a theoretical value for α: identifying $\exp(-\alpha/B)$ with $\exp(-2\pi|\nu|)$ gives $\alpha = \pi/2$.

Introducing the parameter $\beta = 2\pi B/\Lambda$ which, in the above-mentioned computer experiment, served as a measure of the strain gradient, gives the theoretical result:

$$\frac{I_N}{I_0} = e^{-\pi^2/\Lambda\beta}. \tag{36}$$

Comparison of the slope of the curve $\log(I_N/I_0)$ as a function of $1/\beta$ in Balibar, Epelboin & Malgrange (1975) (0·29 μm^{-1}) and of the numerical value of π^2/Λ (0·28 μm^{-1} in that case) shows that theory and 'computer experiments' are in very good agreement.

Conclusion

Penning, who was a pioneer (his thesis goes back to 1966) in the investigation of X-ray propagation in a crystal with a uniform strain gradient, has already mentioned the possibility of interbranch scattering for large values of $|B|$ and even made a conjecture as to the analytical form of the extra wave-field intensity in the frame of the Eikonal theory. The present work differs from his in the fact that the existence of such an extra field has been *demonstrated*, *i.e.* is extracted from Maxwell's equations themselves, by an analysis of the appropriate Green function.

Following this procedure, it has been shown that the 'normal' propagation of a given wave field is perturbed whenever the curvature of its trajectory becomes too strong: a new wave field then appears, precisely in the region of maximum curvature. Our treatment allows an exact calculation of the fraction $e^{-2\pi|\nu|}$ of the original intensity which is transferred to the new wave field. This fraction depends only on the value of the deformation gradient. From which it follows that the reflecting power of a crystal with a uniform strain gradient should differ from that of a perfect crystal by a simple multiplicative factor $e^{-2\pi|\nu|}$.

Still, the present analysis is restricted to the case of a uniform strain gradient, a rather academic situation. The next step should now be to perform the same work assuming a real defect (twin boundary or, even better, a dislocation). This is mathematically more involved. In this respect, the analogy which can be drawn between the present situation and that of scattering by a

potential barrier in quantum mechanics should serve as a starting point for a 'quasi-classical' treatment of the wave-field scattering by a dislocation. This will be, we hope, the object of a further publication.

APPENDIX 1

Here we recall and develop some of the results of the Eikonal theory in view of a further comparison with our own results.

The Eikonal theory deals with the case of a pseudo plane wave, *i.e.* a wave characterized by a given single value η_0 of its deviation parameter but of finite lateral extension. These two characteristics are, in principle, contradictory, since a finite lateral width should result in a finite dispersion $\Delta\eta_0$ in η_0; in spite of this, the concept of a pseudo plane wave is relevant if $\Delta\eta_0 \ll 1$ and it corresponds to the experimental situation of a collimated plane wave.

Trajectories

Penning & Polder (1961), and Kato (1963*b*, 1964) have shown that the energy of such a pseudo plane wave flows, in the crystal, along two hyperbolic trajectories (Fig. 8), the parametric equations of which are:

$$z = \frac{\Lambda}{\pi}(\xi_h + \xi_0) = \frac{\Lambda}{2\pi}\frac{1}{B}(\eta - \eta_0) \qquad (A.1.1)$$

$$x = \frac{\Lambda}{\pi}\,\mathrm{tg}\,\theta(\xi_h - \xi_0)$$

$$= \pm\frac{\Lambda}{2\pi}\frac{tg\theta}{B}(\sqrt{1+\eta^2} - \sqrt{1+\eta_0^2}). \qquad (A.1.2)$$

In (A.1.2) and in the following results the upper sign (lower sign) corresponds to wave field [1] (wave field [2]). Now, if one considers a source point P_0 and a point P inside the crystal (Fig. 9), there exist two possible energy trajectories from P_0 to P. They correspond to two different values of $\eta_{0[1]}$ and $\eta_{0[2]}$ associated with wave fields [1] and [2] respectively. For large values of B, $|\eta_0|$ and

$$|\eta| = |\eta_0 + (2\pi Bz/\Lambda)|,$$

the corresponding hyperbolae reduce to two broken lines (Fig. 10). In this case, $\eta_{0[1]}$ and $\eta_{0[2]}$ reduce to:

$$\eta_{0[1]} = -2B\xi_0 \qquad (A.1.3)$$

$$\eta_{0[2]} = -2B\xi_h. \qquad (A.1.4)$$

Phase change along a trajectory

The general formula for the phase change along a trajectory $P_0 \to P$ is given by Kato (1964, 1974):

$$\Delta\varphi_j(P_0 \to P) = \mathbf{K}_h.\overrightarrow{P_0P} + \chi_0\frac{\Lambda}{\lambda\cos\theta}(\xi_h + \xi_0) + (T - N_h)_{[J]}. \qquad (A.1.5)$$

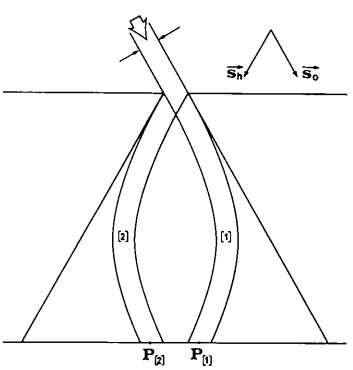

Fig. 8. Optical paths corresponding to an incident pseudo plane wave with a given deviation parameter η_0 in the case $|B| \neq 0$ but $\ll 1$.

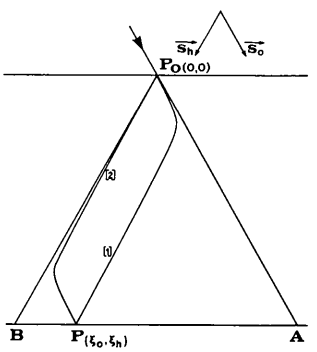

Fig. 9. The incident wave is spherical. $|B| \neq 0$ but $\ll 1$. Given two points P_0 and P, energy is transferred from P_0 to P along any of the two hyperbolic optical paths shown here. These paths correspond to two different values $\eta_{0[1]}$ and $\eta_{0[2]}$ of the parameter η_0.

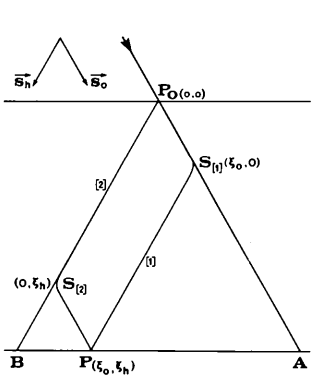

Fig. 10. Incident spherical wave $|B| \neq 0$ and $\gg 1$. The optical paths through which energy is transferred from P_0 to P reduce to two broken lines $P_0S_{[1]}P$ and $P_0S_{[2]}P$. $P_0S_{[1]} = (\Lambda/\pi\cos\theta)\,\xi_0$, $P_0S_{[2]} = (\Lambda/\pi\cos\theta)\,\xi_h$.

$\mathbf{K}_h$ is a constant wavevector linking the reciprocal-lattice point H to the Laue point L_a. The first two terms are purely geometrical factors which do not depend on the deviation parameter or on the strain gradient. We shall drop them hereafter and consider only $(T-N_h)_{[j]}$.

$$T_{[j]} = \pm \frac{\pi}{\Lambda} \int_{P_0}^{P} \frac{dz}{\sqrt{1+\eta^2}} = \pm \frac{1}{2B} |\text{Arg sh } \eta|_{\eta_0}^{\eta_P} \quad (A.1.6)$$

where

$$\eta = \eta_0 + \frac{2\pi B z}{\Lambda}. \quad (A.1.7)$$

$$N_{h[j]} = \tfrac{1}{2}\mathbf{h}.(\mathbf{u}_P - \mathbf{u}_{P_0}) - \frac{1}{2}\int_{P_0}^{P} \frac{1}{\text{tg }\theta}\frac{\partial}{\partial z}(\mathbf{h}.\mathbf{u})\,dx + \text{tg }\theta \frac{\partial}{\partial x}(\mathbf{h}.\mathbf{u})\,dz \quad (A.1.8)$$

with

$$\mathbf{h}.\mathbf{u} = 4B\xi_0\,\xi_h = \frac{B\pi^2}{\Lambda^2}\left(z^2 - \frac{x^2}{\text{tg}^2\,\theta}\right).$$

(A.1.8) has to be integrated along the trajectory P_0P. After some straightforward manipulations one obtains

$$N_{h[j]} = 2B\xi_0\,\xi_h + B(\xi_h^2 - \xi_0^2) \pm \frac{1}{4B}\left[2\eta_{0[j]}\sqrt{1+\eta^2} - (\eta\sqrt{1+\eta^2}) + \text{Arg sh }\eta\right]_{\eta_{0[j]}}^{\eta_{P[j]}} \quad (A.1.9)$$

In the limit $|\eta_{0[j]}| \gg 1$

and $$|\eta_{p[j]}| = \left|\eta_{0[j]} + \frac{2\pi B z}{\Lambda}\right| \gg 1,$$

one obtains (using A.1.2):

$$[T - N_h]_{[j]} = -2B\xi_0\,\xi_h + B(\xi_0^2 - \xi_h^2) - \eta_{0[j]}(\xi_h - \xi_0) \pm \frac{1}{4B}(\eta_{p[j]}|\eta_{p[j]}| - \eta_{0[j]}|\eta_{0[j]}|). \quad (A.1.10)$$

Under the conditions:

$$B > 0\ (B < 0)$$

and $$\eta_{0[j]} < 0\ (>0);\ \eta_{p[j]} > 0\ (<0);$$

$$\frac{1}{4B}(\eta_p|\eta_p| - \eta_0|\eta_0|) = \frac{1}{4|B|}(\eta_p^2 + \eta_0^2) = \tfrac{1}{4}(|Y|^2 + |Y_0|^2), \quad (A.1.11)$$

since $Y = 2v^{1/2}\eta = 2(i/4B)^{1/2}\eta$ [see (3) and (15) in the main text] and

$$[T - N_h]_{[j]} = -2B\xi_0\xi_h + B(\xi_0^2 - \xi_h^2) - \eta_{0[j]}(\xi_h - \xi_0) \pm \left(\frac{|Y|^2}{4} + \frac{|Y_0|^2}{4}\right). \quad (A.1.12)$$

This formula holds also if either η_0 or η is equal to zero since the Arg sh η terms which have been neglected here compared to the terms in η^2 are then equal to zero.

APPENDIX 2

Let us consider an incident plane wave of intensity I_0 with a departure from Bragg angle equal to $\Delta\theta$ and a corresponding η parameter of value η_0.

In order to simplify we assume that the reflecting planes are normal to the crystal surfaces of the crystal (symmetric Laue case). Consequently

$$\eta_0 = \frac{\Delta\theta \sin 2\theta}{C\sqrt{\chi_h\,\chi_{\bar{h}}}}$$

According to the usual Ewald–Laue theory, this plane wave generates in the crystal two wave fields of intensity I_j $(j = 1,2)$ near the entrance surface:

$$I_j = \frac{1}{1+\xi_{j0}^2}, \quad (A.2.1)$$

where

$$\xi_{j0} = D_{hj}/D_{0j} = -\eta_0 \mp \sqrt{1+\eta_0^2} \quad (A.2.2)$$

(upper sign: wave field 1; lower sign: wave field 2).

For a large and negative value of η_0 (as is assumed in this paper)

$$\xi_{10} \simeq -\frac{1}{2|\eta_0|} \text{ and } \xi_{20} \simeq 2|\eta_0| \quad (A.2.3)$$

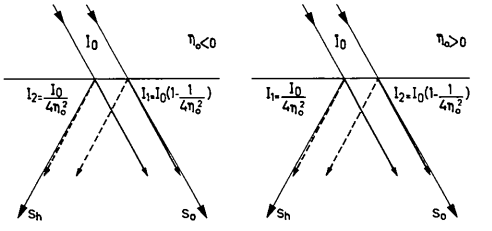

Fig. 11. Splitting of the intensity between wave field 1 and wave field 2 at the entrance surface in the crystal. The wave field which is drawn here in full line is the one into which goes most of the intensity, assuming a large value of $|\eta_0|$, *i.e.* wave field 1 if $\eta_0 < 0$ or wave field 2 if $\eta_0 > 0$.

so that

$$I_1 \simeq 1 - \frac{1}{4\eta_0^2} \simeq 1$$
$$I_2 \sim \frac{1}{4\eta_0^2}. \qquad (A.2.4)$$

For large values of $|\eta_0|$, most of the intensity goes into the wave field which propagates close to $\mathbf{s}_0$: wave field 1 for $\eta_0 < 0$ and wave field 2 for $\eta_0 > 0$ (Fig. 11).

In a case of zero absorption, the intensity is conserved along each wave field. At the exit surface each wave field splits into two waves: the reflected wave (intensity I_R) and the refracted wave (intensity I_T) such that

$$I_{Rj} = \frac{\xi_{je}^2}{1 + \xi_{je}^2} I_j ; I_{Tj} = \frac{1}{1 + \xi_{je}^2} I_j, \qquad (A.2.5)$$

where ξ_{je} is the value of ξ at the exit surface ($\xi_{je} = -\eta_e \mp \sqrt{1 + \eta_e^2}$), η_e being the value of the deviation parameter at the exit surface (Fig. 12). If η_e is large and positive

$$I_{R_1} \simeq I_1 \left(1 - \frac{1}{4\eta_e^2}\right) \simeq I_1$$
$$I_{R_2} \simeq -\frac{1}{4\eta_e^2} I_2. \qquad (A.2.6)$$

If η_e is large and negative

$$I_{R_1} \sim \frac{1}{4\eta_e^2} I_1$$
$$I_{R_2} \sim \left(1 - \frac{1}{4\eta_e^2}\right) I_2 \simeq I_2. \qquad (A.2.7)$$

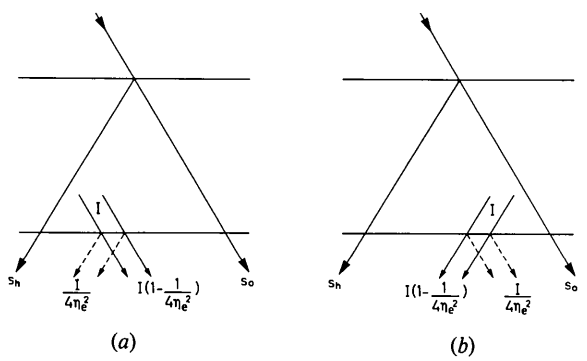

Fig. 12. At the exit surface, each wave field splits into a reflected and a refracted wave. The respective values of the intensities depend on the direction of the wave field in the crystal and consequently on the value of the parameter η at the exit surface, noted here η_e. $|\eta_e|$ is assumed to be large. (*a*) The wave field in the crystal is of type [1] if η_e is <0 or of type [2] if η_e is >0. A very small fraction of the intensity $1/4\eta_e^2$ goes into the reflected wave. (*b*) The wave field in the crystal is of type [1] if η_e is >0 or of type [2] if η_e is <0. A large fraction of the intensity $(1 - 1/4\eta_e^2 \simeq 1)$ goes into the reflected wave.

References

AUTHIER, A. (1961). *Bull. Soc. Fr. Minéral. Cristallogr.* **84**, 115–127.

AUTHIER, A. (1967). *Adv. X-ray Anal.* **10**, 9.

AUTHIER, A. (1977). *Section Topography in X-ray Optics*, edited by H. J. QUEISSER. Berlin: Springer Verlag.

BALIBAR, F. (1968). *Acta Cryst.* A**24**, 666–676.

BALIBAR, F. (1969*a*). *Acta Cryst.* A**25**, 650–658.

BALIBAR, F. (1969*b*). Thesis, Paris.

BALIBAR, F. (1970). *Acta Cryst.* A**26**, 647–654.

BALIBAR, F., EPELBOIN, Y. & MALGRANGE, C. (1975). *Acta Cryst.* A**31**, 836–840.

CHUKHOVSKII, F. N. (1974). *Kristallografiya*, **19**, 482–488.

CHUKHOVSKII, F. N. & PETRASHEN', P. V. (1977). *Acta Cryst.* A**33**, 311–319.

Higher Transcendental Functions (1953). Vol. 1. New York: McGraw Hill.

KATAGAWA, T. & KATO, N. (1974). *Acta Cryst.* A**30**, 830–836.

KATO, N. (1961). *Acta Cryst.* **14**, 627–636.

KATO, N. (1963*a*). *Acta Cryst.* **16**, 276–290.

KATO, N. (1963*b*). *J. Phys. Soc. Jpn*, **18**, 1785–1791.

KATO, N. (1964*a*). *J. Phys. Soc. Jpn*, **19**, 67–77.

KATO, N. (1964*b*). *J. Phys. Soc. Jpn*, **19**, 971–985.

KATO, N. (1974). In *X-ray Diffraction*, edited by L. V. AZAROFF. New York: McGraw Hill.

LITZMAN, O. & JANACEK, Z. (1974). *Phys. Status Solidi A*, **25**, 663–665.

PENNING, P. (1966). Thesis, Eindhoven.

PENNING, P. & POLDER, D. (1961). *Philips Res. Rep.* **16**, 419–440.

TAKAGI, S. (1969). *J. Phys. Soc. Jpn*, **26**, 1239–1253.